

OPTICAL PROPERTIES OF SILVER NANOWIRES CONJUGATED WITH PROTEIN

DO THI NGA^{1,†}, VU VAN HUY^{2,3} AND CHU VIET HA³

¹*Institute of Physics, Vietnam Academy of Science and Technology
10 Dao Tan, Ba Dinh, Hanoi, Vietnam*

²*Hai Duong Central College of Pharmacy, Vietnam*

³*Faculty of Physics, Thai Nguyen University of Education, Thai Nguyen, Vietnam*

E-mail: [†]dtnga@iop.vast.ac.vn

Received 7 January 2021

Accepted for publication 26 April 2021

Published 14 May 2021

Abstract. *Optical properties of protein-conjugated metallic nanowires are theoretically investigated based on the Mie theory and the core-shell model. Our numerical calculations show that optical spectra of protein-conjugated nanowires can have more a maximum compared to these nanowires without biomolecules. This finding is in a good agreement with previous experiments. We provide better interpretation for the origin of optical peaks in absorption spectrum of nanowires. Our results can be used for designing biosensors and bio-detectors.*

Keywords: optical properties; silver nanowires; BSA, biosensors; bio-detectors.

Classification numbers: 78.20.Bh, 78.67.Uh.

I. INTRODUCTION

In recent years, plasmonic properties of silver nanowires are of great interest because they have various potentially technological applications. The strong interaction of silver nanowires with electromagnetic field can be exploited to enhance the efficiency in a solar cell [1, 2]. Silver nanowire network placed on glass substrate can significantly increase optical transmittance. This optical property can be tuned by varying nanowire density and shape [3, 4]. Nanowires are long, so it is easier to control number of nanowires in solution than other kinds of nanostructures. Silver nanowires have been applied in the field of printed electronics with low signal loss at high-frequency radio [5]. In 2014, Sheldon and his workers successfully designed an plasmoelectric

device with functions as an optical-to-electrical converter based on silver nanoparticles [6]. Therefore, silver nanowires can be also exploited to develop next-generation optoelectronic devices that have high efficiency for conversion from optical to electrical energy.

Bovine serum albumin (BSA) protein has been widely used in the field of biophysics and medical science. BSA proteins are vehicle for delivering nanostructures to localtions of unhealthy cells [7, 8]. Coating BSA on metallic nanoparticles can stabilize them and avoid aggregation of nanoparticles [9]. Biological configuration and physical properties of BSA protein dramatically vary with environmental changes [10]. Thus, combining BSA protein and nanostructures can propose state-of-the-art biosensors.

Optical peak of BSA-conjugated gold and silver nanowires in visible regime can be exploited in a variety of applications: detecting protein BSA in environment and estimating the number of adsorbed proteins BSA on metallic nanocylinders. Nanowires can absorb optical energy from incident laser light to heat up and destroy these cells. An increase of temperature is strongly dependent on an intensity and absorbance of laser. The mechanism is based on the photothermal effects, which has been intensively investigated for cancer treatment studies. Previous studies showed that this effect can raise temperature of nanowires to 353 K. At this temperature, most proteins melt and desorb from metallic structures.

In this work, we theoretically study the optical properties of silver nanowires using the Mie theory and effective medium approximation. Silver nanowires are dispersed in an aqueous BSA protein solution. BSA molecules attach on silver nanowires via van der Waals interaction and form a protein monolayer on the surface. Therefore, we can observe a conjugation between protein BSA and silver nanowires. However, protein BSA cannot cover 100 % surface of metallic nanostructures because of repulsive Coulomb force [9, 10].

II. THEORETICAL BACKGROUND

Calculating exactly the number of BSA molecules on gold nanoparticle's surface based on the absorption spectrum and the extended Mie theory [9] suggests that the core-shell model and the effective medium approximation provide a good agreement between theoretical calculations and experiments for spherical nanoparticles. Now, we apply these theories to the nanowire system to investigate and predict properties of protein-conjugated silver nanowires. An idea of modeling biological molecules conjugated nanowire as a core-shell structure has been widely used [11] and can be depicted in Fig. 1. There, r_1 is the radius of nanowires and $(r_2 - r_1)$ is the thickness of the protein coating layer.

For very thin and infinitely long cylinder ($kr_2 = 2\pi r_2/\lambda \ll 1$), the scattering and absorption efficiency, defined by the normalization of the scattering and absorption cross sections to the area πr_2^2 , at a wavelength λ is calculated via the expressions [12]

$$\begin{aligned} Q_{scat} &= \left(\frac{2\pi}{\lambda} \sqrt{\epsilon_m} \right)^3 r_2^2 (|\alpha_0|^2 + |\alpha_1|^2), \\ Q_{abs} &= \frac{2\pi}{\lambda} \sqrt{\epsilon_m} \text{Im}(\alpha_0 + \alpha_1), \end{aligned} \quad (1)$$

where ϵ_m is the dielectric constant of medium, Q_{scat} and Q_{abs} correspond to the scattering and absorption efficiency of the system, respectively. Note that if one considers larger proteins so that the assumption $2\pi r_2/\lambda \ll 1$ is not valid, the predictive validity of the Gans-Mie theory is reduced.

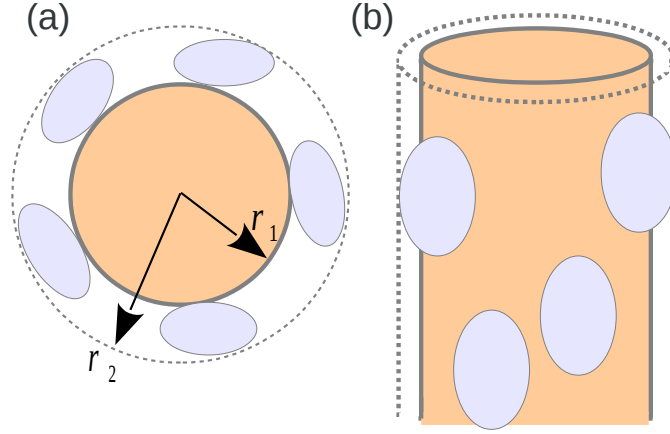


Fig. 1. (Color online) Schematic illustration for (a) side view and (b) top-down view of the core-shell model for protein-conjugated metallic nanowires.

Thus, it is important to check a ratio of r_2 to incident wavelength before using the approach. From these, we can determine the extinction efficiency $Q_{ext} = Q_{abs} + Q_{scat}$. α_0 and α_1 are given by

$$\alpha_0 = \frac{\pi r_2}{2} \left[\frac{1}{8} (kr_2)^2 (\varepsilon - \varepsilon_m) + \frac{\varepsilon - \varepsilon_m}{\varepsilon_m \left[1 + \frac{\varepsilon}{2} (kr_2)^2 \log(kr_2 \sqrt{\varepsilon_m}) - \frac{i\pi}{4} (kr_2)^2 (\varepsilon - \varepsilon_m) \right]} \right],$$

$$\alpha_1 = \frac{\pi r_2}{2} \left[2 \frac{\varepsilon - \varepsilon_m}{\varepsilon + \varepsilon_m} + \frac{1}{4} (kr_2)^2 (\varepsilon - \varepsilon_m) \right], \quad (2)$$

where ε is the dielectric function of the core-shell cylinder.

An effective dielectric function of core-shell nanocylinder dispersed in a solution can be found from the Maxwell-Garnett theory as

$$\varepsilon_a = \varepsilon_1 \left[1 + 2 \left(\frac{r_1}{r_2} \right)^2 \right] + 2\varepsilon_2 \left[1 - \left(\frac{r_1}{r_2} \right)^2 \right],$$

$$\varepsilon_b = \varepsilon_1 \left[1 - \left(\frac{r_1}{r_2} \right)^2 \right] + \varepsilon_2 \left[2 + \left(\frac{r_1}{r_2} \right)^2 \right],$$

$$\varepsilon = \varepsilon_2 \varepsilon_a / \varepsilon_b, \quad (3)$$

where ε_1 and ε_2 are the dielectric function for the core (Au/Ag), shell (BSA + surrounding medium), respectively. Parameters and analytical expressions for these dielectric functions can be taken from the previous study [9]. We introduce the filling factor of protein BSA on metallic surface f , $\varepsilon_2 = f\varepsilon_{protein} + (1-f)\varepsilon_m$ [9]. The dielectric function of ε_m is taken from experimental data in Ref. [13]. Meanwhile, the analytical expression of $\varepsilon_{protein}$ was previously reported [9].

III. NUMERICAL RESULTS AND DISCUSSIONS

Figure 2 shows the real and imaginary dielectric function of protein BSA. $\text{Re}[\epsilon_{protein}]$ and $\text{Im}[\epsilon_{protein}]$ monotonically decreases with an increase of λ . Although $\epsilon_{protein}$ of this protein exhibits several oscillators [9], there is no resonance frequency in the visible range.

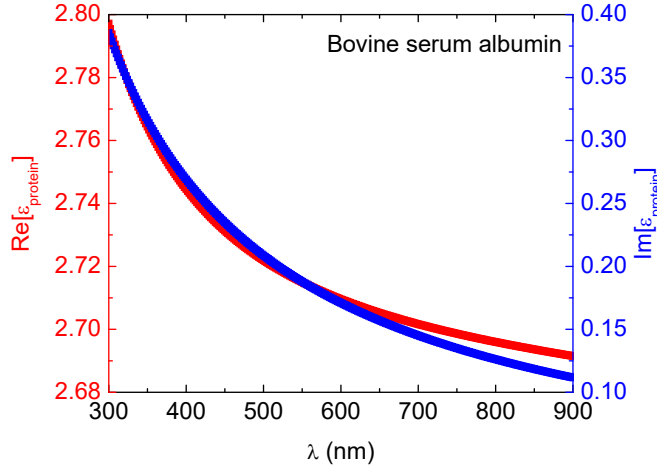


Fig. 2. (Color online) Imaginary and real parts of $\epsilon_{protein}$ as a function of wavelength.

Figure 3 shows the absorption and extinction efficiency of BSA-conjugated silver nanocylinder in water with different filling factors. Previous studies [9, 10] pointed out that protein molecules attach to gold nanoparticle surface and form only a layer but do not cover fully the surface ($f = 0.4$) because BSA molecules repel each other via the repulsive Coulomb force. In this research, therefore, we calculate the optical spectrum with $f = 0.2, 0.4$ and 0.6 . $f = 0$ corresponds to the case of no protein adhering on cylinder and the curve of the extinction efficiency has a peak and is similar to the optical spectrum of silver nanocylinder in vacuum [12, 14], except that the intensity in water is higher. It is well-known that we can observe two maxima in the absorption spectrum of metallic nanorods due to the transverse and longitudinal plasmon oscillations. The length of nanowires, however, is considered as infinity, so only a peak at around 390 nm caused by the transverse mode in solution without biological molecules can be obtained.

Protein layer on silver surface has significant effect on optical spectra. As can be seen in Fig. 3, the protein-conjugated silver nanowire has an additional peak compared to pure silver nanowire. This finding is similar to previous experimental results [15]. Han and Lee showed that the extinction spectrum of poly(sodium 4-styrenesulfonate) (PSS) molecules on the surface of a very long silver nanowire has two maxima. The first peak at 409 nm corresponds to the transverse surface plasmon resonance and the second plasmonic resonance is at the range of 500-600 nm. Another recent experimental study [16] also reported the presence of the second peak in the absorption spectrum of silver nanowires in approximately 700 nm. However, the longitudinal mode cannot be responsible for second peak as the authors argued because the aspect ratio is

approximately 50, the position of the longitudinal plasmon peak is beyond the visible and near-infrared regime [16, 17]. This peak can be interpreted as the binding between biomolecules or a ligand layer and silver nanowires. It is not the resonance frequency of BSA protein since this protein does not have any optical peak in this range of wavelength (as shown in Fig. 2).

In most experiments for metallic nanorods coated by BSA proteins [18], the aspect ratio is around 2-4, the resonances originating from the longitudinal plasmon mode and the metal-BSA interaction are in the same region of wavelength, or the adsorption of biological molecules is not enough to affect the optical spectrum. These two peaks, therefore, are overlap and it is hard to separate two components.

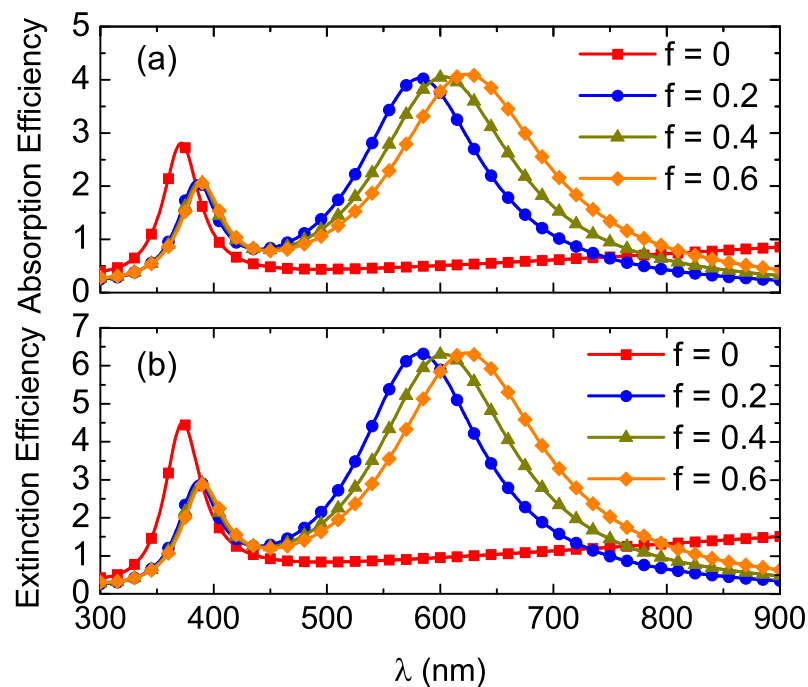


Fig. 3. (Color online) The absorption and extinction efficiencies of silver nanocylinder in water with different adsorption of protein BSA on surface. The diameter of silver cylinder in the calculations is 20 nm.

Figure 3 also presents that the absorption efficiency of silver nanowires plays an important role in the extinction efficiency when $r_1 = 10$ nm. The contribution of Q_{scat} to Q_{ext} almost disappears at $r_1 = 8$ nm since $Q_{scat} = Q_{ext} - Q_{abs}$. Recall that the scattering process becomes more comparable or larger than the absorption process when the size of nanostructure is large. For metallic spherical nanoparticles, effects of scattering efficiency cannot be ignored when the value of radius is much larger than 60-nm radius.

Another way to investigate the localized surface-plasmon resonance of nanowire is considering such material as an ellipsoidal nanoparticle or a spherical prolate spheroid [19, 20]. In this case, a semi-major axis (a) is much longer than a semi-minor axis (b and c), here ($a > b = c$). The

absorption cross section of the spheroid can be calculated using the Mie-Gans theory [12]

$$Q_{abs} = \frac{2\pi V \varepsilon_m^{3/2}}{3\lambda} \sum_{k=a,b,c} \frac{1}{P_k^2} \frac{\varepsilon_2(\omega)}{\left[\varepsilon_1(\omega) + \frac{1-P_k}{P_k} \varepsilon_m \right]^2 + \varepsilon_2^2(\omega)}, \quad (4)$$

where $\varepsilon(\omega) = \varepsilon_1(\omega) + i\varepsilon_2(\omega)$ is the effective dielectric function of object calculated by Eq. (2), $\varepsilon_2(\omega)$ is the imaginary part of $\varepsilon(\omega)$, ε_m is the dielectric constant of medium, $V = 4\pi abc/3$ is the volume of the oblate prolate and λ is the wavelength of the incident light. A geometrical factor determined for the prolate shape is expressed by

$$P_a = \frac{1-e^2}{2e^3} \left[\ln \left(\frac{1+e}{1-e} \right) - 2e \right], \quad (5)$$

where $e = \sqrt{1-\eta^2}$ and $\eta = c/a$. Since $b = c$, so $P_b = P_c = (1-P_a)/2$. Importantly, in the case of cylinder, $a \gg b = c$. Thus, $e = 1$, $P_a = 0$ and $P_b = P_c = 1/2$. This approach gives clear and good explanation why the peak in the absorption spectrum of nanocylinder is due to the transverse mode. Eq. (4) can be recast as

$$Q_{abs} = \frac{16\pi V \varepsilon_m^{3/2}}{3\lambda} \frac{\varepsilon_2(\omega)}{[\varepsilon_1(\omega) + \varepsilon_m]^2 + \varepsilon_2^2(\omega)}, \quad (6)$$

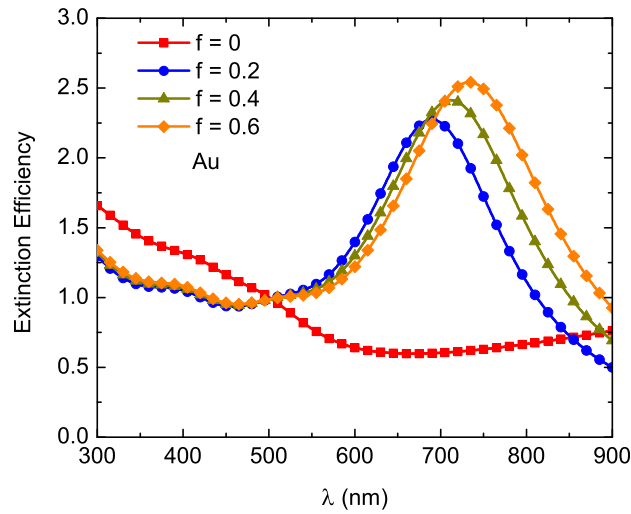


Fig. 4. (Color online) The extinction efficiency of gold nanocylinder in water with different adsorption of protein BSA on surface. The diameter of nanowires in the calculations is 20 nm.

Two theories have a good agreement that maxima of the absorption spectrum of nanowires exhibit at $|\varepsilon(\omega) + \varepsilon_m| = 0$ [12]. While the localized surface plasmon resonance of a spherical

nanoparticle is at $|\varepsilon(\omega) + 2\varepsilon_m| = 0$ [12]. Thus, there is a possibility that surface plasmon resonances in other plasmonic nanocylinders can be shifted from the visible range. To confirm this argument, we carry out theoretical calculation for the extinction efficiency of 20-nm gold nanocylinders and show numerical results in Fig. 4. Clearly, gold nanocylinders have no optical peak in visible range. This method reveals that for silver nanowires with large aspect ratio (≥ 40), the longitudinal mode can be totally ignored. As a result, it is impossible to attribute the optical peak in the range of 500-700 nm when proteins are coated on the metal surface due to the longitudinal plasmon.

In addition to BSA protein, our theoretical approach can be applied to other proteins/molecules such as protein A/G and goat anti-mouse immunoglobulin G (IgG) in Ref. [21]. We need to know either analytical functions or experimental data of frequency-dependent dielectric of biological molecules. Recently, some alternative plasmonic materials such as TiN, TaN, and ZrN [22] have been widely studied. Optical properties of these materials are similar to noble metals when prepared in the same size and structures. Thus, it is possible to replace gold and silver in our biosensors with the alternative plasmonic materials.

IV. CONCLUSIONS

In conclusion, we have presented a comprehensive explanation for optical peaks of BSA-conjugated silver nanowires. The transverse plasmon mode is fully responsible for the optical resonance at 390 nm. The peak at 600 nm is due to biological molecules binding on nanowires and strongly depends on the dielectric function of protein and the adsorption of protein on silver nanowires.

ACKNOWLEDGMENT

This research was funded by Vietnam National Foundation for Science and Technology Development (NAFOSTED) under grant number 103.01-2018.337.

REFERENCES

- [1] C.-H. Kim, S.-H. Cha, S. C. Kim, M. Song, J. Lee, W. S. Shin, S.-J. Moon, J. H. Bahng, N. A. Kotov and S.-H. Jin, *ACS Nano* **5** (2011) 3319.
- [2] Y. Yang, X. Lin, J. Qing, Z. Zhong, J. Ou, C. Hu, X. Chen, X. Zhou and Y. Chen, *Appl. Phys. Lett.* **104** (2014) 123302.
- [3] S. Xie, Z. Quyang, N. Stokes, B. Jia and M. Gu, *J. Appl. Phys.* **115** (2014) 193102.
- [4] D. A. Dinh, K. N. Hui, K. S. Hui, P. Kumar and J. Singh, *Rev. Adv. Sci. Eng.* **2** (2013) 324.
- [5] N. Komoda, M. Nogi, K. Suganuma, K. Kohno, Y. Akiyama and K. Otsuka, *Nanoscale* **4** (2012) 3148.
- [6] M. T. Sheldon, J. v. de Groep, A. M. Brown, A. Polman, H. A. Atwater, *Science* **346** (2014) 828.
- [7] L. Yang, H.-J. Wang, H.-Y. Yang, S.-H. Liu, B.-F. Zhang, K. Wang, X.-M. Maa and Z. Zhengb, *Chem. Commun.* (2008) 2995.
- [8] A. Loureiro, A. S. Abreu, M. P. Sárria, M. C. O. Figueiredo, L. M. Saraiva, G. J. L. Bernardes, A. C. Gomesb and A. Cavaco-Paulo, *RSC Adv.* **5** (2015) 4976.
- [9] Anh D. Phan, Trinh X. Hoang, Thi H. L. Nghiem and Lilia M. Woods, *Appl. Phys. Lett.* **103** (2013) 163702.
- [10] D.-H. Tsai, F. W. DelRio, A. M. Keene, K. M. Tyner, R. I. MacCuspie, T. J. Cho, M. R. Zachariah and V. A. Hackley, *Langmuir* **27** (2011) 2464.
- [11] T. Fujigaya and N. Nakashima, *Sci. Technol. Adv. Mater.* **16** (2015) 024802.
- [12] Michael Quinten, *Optical Properties of Nanoparticle Systems*, Wiley, Weinheim, Germany (2011).
- [13] G. M. Hale and M. R. Querry, *Appl. Opt.* **12** (1973) 555.

- [14] M. N' Gom, J. Ringnalda, J. F. Mansfield, A. Agarwal, N. Kotov, N. J. Zaluzec and T. B. Norris, *Nano Lett.* **8** (2008) 3200.
- [15] S. H. Han and J.-S. Lee, *Langmuir* **28** (2012) 828.
- [16] W. Zhou, A. Hu, S. Bai, Y. Maa and D. Bridges, *RSC Adv.* **5** (2015) 39103.
- [17] M. A. Bates and D. J. Frenkel, *J. Chem. Phys.* **112** (2000) 10034.
- [18] E. Yasun, C. Li, I. Barut, D. Janvier, L. Qiu, C. Cui and W. Tan, *Nanoscale* **7** (2015) 10240.
- [19] T. Igarashi, H. Kawai, K. Yanagi, N. T. Cuong, S. Okada and T. Pichler, *Phys. Rev. Lett.* **114** (2015) 176807.
- [20] E. Mercado, S. Santiago, L. Baez, D. Rivera, M. Gonzales, M. E. Riversa-Ramos, M. Leon, M. E. Castro, *Nanoscale Res. Lett.* **6** (2011) 602.
- [21] Daniel Rodrigo, Odeta Limaj, Davide Janner, Dordaneh Etezadi, F. Javier Garcia de Abajo, Valerio Pruneri and Hatice Altug, *Science* **349** (2015) 165.
- [22] Gururaj V. Naik, Vladimir M. Shalaev and Alexandra Boltasseva, *Adv. Mater.* **25** (2013) 3264.